Age of Information in Molecular Communication Channels

Jorge Torres Gómez, Ketki Pitke, Lukas Stratmann, Falko Dressler*

School of Electrical Engineering and Computer Science, TU Berlin, Germany

Abstract

Molecular communication (MC) is gaining increasing popularity for data communication between nano systems. First applications both in the biomedical and the industrial domain show that MC is often better suited than conventional radio communication. Theoretical studies regarding the communication capabilities are accounting for information-theoretic metrics to maximize the system performance concerning the communication rate, the bit error rate, and the delay. However, the freshness of status updates by means of MC is still a topic to be addressed in this field. The concept of the age of information (AoI) has been introduced to particularly analyze and design timely system updates when considering the limited capabilities of the underlying communication channel. In this paper, we introduce the AoI concept in molecular communication channels. In particular, we focus on the peak age of information (PAoI), which describes the maximum AoI on a per packet basis. We derive a theoretical equation to compute the average PAoI metric. This allows analyzing the trade-off between an increased rate of transmission (thereby a reduced latency) and the produced inter-symbol interference (ISI) (thereby an increased error rate). We further validate our analytical results by means of simulation and illustrate the impact of the channel parameters. We finally summarize open research problems to conclude the discussion of AoI in the field of MC.

Key words: Molecular Communication, Age of Information, Performance Metrics, Channel Characterization

1. Introduction

Molecular communication (MC) mechanisms are recently addressed as particularly suited to support nanonetwork communication applications. The use of molecules and particles as carriers of information has proven to be better suited than the conventional use of electromagnetic waves in the nano- [3, 41] and macroscale [27, 28] ranges. Because of their bio-compatible nature, the use of molecules and particles exhibits robust and energy-efficient (low heat dispersion) properties that becomes rather suitable to devise communication schemes by molecular means. We have seen very successful approaches to MC ranging from theoretical channel analysis to new MC devices [52].

Currently, visionary applications are being developed using MC and also supported by synthetic biology components [51]. Particularly, the early detection and treatment of diseases is of interest when, for example, designing smart drugs mechanisms, tissue engineering, genetic engineering, treatment of cancer, and lab-on-a-chip devices [23, 47, 10]. Additionally, industrial applications are also foreseen [29, 28]. The communication in the confinement of some industrial environments like pipe networks for oil, water, and gas pipelines, where electromagnetic waves will be highly attenuated, can be supported by MC techniques as well.

A variety of propagation models are also reported for MC. Examples include diffusion, flow assisted, active transportation using molecular motors, or bacterial propagation mechanisms [21]. However, the MC channels introduce singular barriers to implement communication systems. One major difference compared to conventional radio communication is that information carriers are constituted by particle entities that interact with the medium in their travel from source to destination. The trajectory is not necessarily straight, but impacted by chemical and mechanical interactions [44]. A released particle in a diffusive medium will randomly move until reaching a given destination [8]. Consequently, the propagation delay will be considerably larger or infinite. In contrast to the emission of waves, it is not certain that the emission of particles reaches the destination even for short distances and line of sight conditions. Furthermore, when considering the emission of a group of molecules, remaining particles from the previous emission may produce a high inter-symbol interference (ISI), which in turn will degrade the performance.

In this communication scenario, the main metrics used to assess the performance of MC systems focus on maximizing the system performance. Relying on theoretical analysis, simulators, and first wet-lab experiments the motif is to improve the achievable channel capacity, observed delays, and the resulting symbol and packet error proba-

---

*Corresponding author.

Email addresses: `torres-gomez@ccs-labs.org` (Jorge Torres Gómez), `pitke@ccs-labs.org` (Ketki Pitke), `stratmann@ccs-labs.org` (Lukas Stratmann), `dressler@ccs-labs.org` (Falko Dressler)

bility. However, the analysis of the achievable *freshness of information* is still a topic to be addressed in this field, which becomes particularly important when considering the cooperation of nano devices to overcome their limited resources as individual units.

We suggest to use the concept of age of information (AoI) and its corresponding metrics as a more suitable tool to analyze and design such nano communication scenarios. The perceived AoI [58] of the received packets will provide a metric to analyze the performance regarding the timeliness of updates in molecular communication systems. In contrast to the reported studies, that evaluates the transmission rate to improve throughput [42], or to reduce delay [54], and the impact of errors [48] separately, the use of the AoI concept allows to jointly consider all in the same theoretical framework. Consequently, a better tradeoff can be achieved when minimizing the perceived age regarding the status updates. In the context of MC, such an analysis is still pending to address.

In this paper, we provide the first evaluation of the age of information concept in molecular communication channels. We consider the conventional discrete-time channel model due to its simplicity and wide applicability to describe the molecular channels. In particular, we look at the so-called peak age of information (PAoI) and the average PAoI, which describe the maximum age of information per packet and the average of this for an ongoing communication, respectively. We present preliminary results for the very popular diffusion model. Our main contributions can be summarized as follows:

- We introduce, for the first time, the use of age of information in MC scenarios. We outline and discuss the potentials of using AoI as a key metric in the MC field.

- We derive a closed-form expression to compute the PAoI based on reported MC models and receivers.

- We introduce preliminary ideas regarding the system utilization for the optimal average PAoI and also discuss future research challenges.

The remainder of the paper is structured as follows. Section 2 recapitulates necessary background on molecular communication. Section 3 describes how the concept of age of information can be applied to MC. This section also shows how to theoretically derive the average PAoI metric in MC channels. Section 4 shows some first simulation results to confirm the correctness of the theoretical average PAoI. The simulation results also illustrate the impact of MC design parameters in the status updates regarding the varying distance between the transmitter and the receiver, the varying receiver radius, and the diffusion coefficient. Section 5 summarizes open research problems regarding the AoI metrics in MC channels. Finally, Section 6 concludes the paper.

2. Molecular Communication – A Primer

In spite of the reported benefits, the MC channels impose particular characteristics in comparison to the electromagnetic field when analyzing the propagation of molecules. In contrast to the Friis free space model for the electromagnetic wave propagation [49], in the MC channels the propagation is governed by mechanical and chemical interactions between the released molecules and the medium. As a consequence, the time of propagation for a single molecule will be proportional to the square of the distance, which in turn will introduce a high propagation delay on the macroscopic distance [8]. For instance, a small molecule in the water at room temperature will diffuse through a $1\,\text{cm}$ distance in $14\,\text{h}$ [8]. This is highly contrasting with the achievable speed of electromagnetic waves in water, where the same distance will be covered in just $44\,\text{ps}$.

On the other hand, MC channels are typically high spreading mediums. For example, a pulse wave of one second can be spread larger than twice when using particles with a diffusion coefficient around or less than $100\,\mu\text{m}^2/\text{s}$ (e.g., microRNA in water[1]) [8]. These high spreading effects experienced in the MC channels will correspondingly produce a high ISI for the regular transmission of pulses, which in turn will limit the achievable rate of transmissions.

These particularities regarding the MC channels impose new challenging restrictions when addressing the implementation of modulation schemes, error-correcting codes, as well as reception and detection mechanisms to implement communication systems in the MC environment. These different fields are typically conceived to optimize system utilization metrics like bit error rate (BER), delay, and the achieved capacity through the theoretical conception of MC channel models [35].

In the macroscale range, artificial MC systems are reported to be implemented through commercially available sensors and bio-inspired techniques. Instead of the rather expensive nanoengineering components, middle-range distances ($\sim 3\,\text{m}$) have been achieved through the use of pheromones (biological approach), chemical elements (like Calcium ions, Di-nitrogen, Acetone, Alcohol, Methanol), or magnetic particles. Supported by a flow to induce drift on the molecules or particles, several experimental setups are built through a variety of carrier elements through air-based and micro-fluid mediums. This is the case of alcohol molecules emitted with electrical sprayers and received with alcohol sensors [19], also extended to multiple input and multiple output (MIMO) [31], pH-level controllers with pH sensors [20], magnetic nanoparticle emissions using a comparably big susceptometer receiver [55], passive receivers supported by external magnetic fields [56], and odor generators with a mass spectrometer [39].

To transmit, the information is typically encoded in the number of released molecules, molecule type, or the

---

[1]Search BioNumbers – The Database of Useful Biological Numbers, https://bionumbers.hms.harvard.edu/search.aspx

molecular release time [35, 32]. The implemented modulations are commonly reported as pulse-based following the natural biological processes where information is interchanged by means of pulse sequences [25]. A single molecule type is used to implement simple modulation mechanisms regarding the concentration of molecules as on-off keying (OOK), concentration shift keying (CSK), or amplitude shift keying (ASK). Complex modulation mechanisms are implemented through multiple molecule types like molecular shift keying (MoSK), depleted molecular shift keying (D-MoSK), or isomer-based ratio shift keying (IRSK), and present a better performance regarding the impact of ISI [34]. Concerning the time of emission, pulse position modulation (PPM) [25] and release time shift keying (RTSK) [17] are two reported modulations. PPM presents a reduced performance regarding range and throughput in comparison to the concentration-based modulations, while the asynchronous modulation RTSK exhibits an improved communication rate [21]. Furthermore, in addition to single-carrier modulations, multiple-carrier waveforms have also been reported [15] as the orthogonal frequency division multiplexing (OFDM) with a reduced impact of the ISI produced by the MC channels.

In order to reduce errors due to ISI, the sequence to be transmitted can be encoded first. By including redundant bits in the transmitted sequence, conventional and a variety of novel techniques have been devised. The conventional codes are given by Hamming, Convolutional, Turbo, or low-density parity-check (LDPC) codes on one hand. On the other hand, new reported codes are the ISI-free coding, molecular coding (MoCo) distance function, Hamming minimum energy code (MEC), and self-orthogonal convolutional codes (SOCCs) [35]. However, results exhibit a superior performance regarding the conventional coding techniques. On the nanoscale, this is the case of the Hamming and LDPC codes, in the middle-range the LDPC codes present the best performance, while in the long-range the best code is the Convolutional scheme [35].

The propagation of the carrier molecules is also analyzed for the diffusive, advective, and degradative mediums [29], where their channel impulse response (CIR) is derived to account for the received sequence of molecules. In addition, the propagation can be implemented by molecular motors comprised of multi-component protein molecules where the information is carried in a more protected environment. Concerning the reception mechanisms, a variety of theoretical studies have been conducted to model ideal and practical receivers. Ideal receivers, when considering a perfect absorber with a spherical geometry [46], are the most widely used because they avoid the impact of the receiver mechanisms in the analysis of the propagation of molecules.

The detection mechanisms are implemented by sampling and energy-based mechanisms. The sampling-based detectors sample the receiver concentration of molecules according to a given sampling period [36]; they are able to implement the current detection by using the previous output. On the other hand, the energy-based detectors are based on the collected total number of molecules during a predefined time interval [37]. Their complexity to implement is less than the sampling detectors because of the avoiding of memory blocks to store the previously decoded symbols. However, sampling detectors are more robust because of the implemented parameter estimation techniques to mitigate the impact of ISI.

In order to develop and fine-tune above communication schemes, having appropriate simulation tools is important. They have the potential to reduce material costs and facilitate larger parameter studies compared to using a physical testbed only. There exist different approaches for the simulation of MC channels, each with their own advantages and disadvantages depending on the scenario. For instance, these approaches include the following simulation scenarios: NanoNS3 [30] with very low computation costs and the capability to explore higher-layer protocols such as routing; BiNS2 [22] which allows configuring the environment more freely, AcCoRD [43] with included computationally efficient mesoscopic domains, and the Pogona simulator [9, 16] that re-uses the output of existing computational fluid dynamics simulator accounting for accurate propagation models.

So far, the main metrics on the reported studies for the communication systems through MC channels (theoretical and through the use of simulators) focus on maximizing the utilization of the system regarding achievable channel capacity, delay, and error probability. However, the analysis of the achievable freshness of information is still a topic to be addressed in this field. To overcome their limited resources as individual units, nanodevices are expected to cooperate with each other [2]. In this scenario, it will be of major importance to evaluate a timely awareness regarding the status of remote sensors or the complete system as a network.

Regarding the timely update of samples, implicitly it has been addressed by some reported studies when computing the achievable transmission rate on the transmitter side to account for the improved performance. For instance, the symbol-period is derived considering the saturation point of receivers [38]. This is to avoid the excessive arrival of molecules, which will be limited to be removed by the detector. Other reports compute the symbol-period that minimizes the error probability to decode the transmitted sequence as in [48]. Additionally, there are transmission protocols (regarding the symbol duration) designed to maximize the mutual information in deformable cellular tissues [6]. These transmission protocols are also analyzed by considering static and dynamic time slot durations to improve the data rate.

Furthermore, the trade-off between the rate of transmissions and delay have been characterized in [54] regarding a pair of communicating devices with a relay node. This trade-off is evaluated and analyzed when an M/D/1 FIFO [2] queue is implemented in the relay node to account for the

---

[2]M/D/1 accounts for a system having one server, time of arrival

future study of the optimal settings. The rate of transmission is also analyzed to improve the system efficiency [42]. Efficiency is measured by the ratio between throughput (total number of molecules processed by the receiver) and the total number of emitted molecules (on the transmitter side). The improved efficiency will account for saving resources regarding the emitted molecules. Those molecules that cannot be processed on the received side will diffuse away or will remain in the environment interacting with future emissions, thereby increasing the channel noise.

These above reports characterize the trade-off between transmission rate and system performance metrics such as BER or delay. At the same time, the AoI concept provides a framework to jointly capture these trade-offs, and to account for a system optimally updated instead. In this paper, we provide a first evaluation of the AoI in MC channels. Although widely analyzed in conventional communication schemes, the fundamental limits regarding the status update can also be analyzed when molecules are the carriers instead of waves. To illustrate the obtaining of the AoI metric, we consider the conventional discrete-time channel model due to its simplicity and wider applications to describe the molecular channels.

3. Age of Information of Molecular Communication Channels

In analogy to information theory principles, the transmission of information through molecular communication channels is modeled by considering the three main constituting elements, namely the transmitter, the medium, and the receiver. Each of these elements is modeled by their specific restrictions to account for realistic scenarios or by ideal assumptions (although non-realistic to account for a wider theoretical analysis). Here, we follow the second approach as a first step in deriving a closed-form expression to evaluate the average AoI and provide an overview regarding the freshness of the received information packets. For ease of analysis, here we consider that a packet is comprised of the information-bits carried by one symbol when transmitted through the MC channel.

Considering that AoI metrics are an end-to-end descriptor, to compute these values we must consider the MC channel by its end-to-end model (Section 3.1) as well as the detection mechanisms (Section 3.2). The end-to-end models will account for the expected total number of received molecules through the medium, the detection mechanisms for their proper detection. We will further consider the general concerns regarding the AoI metrics in Section 3.3 to compute the average PAoI for the MC channel case (Section 3.4). We reveal the trade-off mechanism between the desired increase of the rate of transmission (reduced

latency) and the non-desirable effect regarding the impact of ISI when accounting for the average PAoI. Finally, we address an optimal condition for the rate of transmission to minimize the average PAoI (Section 3.5).

3.1. Discrete Molecular Communication Channel Models

Several models are reported for each constitutive element regarding the transmitter-medium-receiver chain, as depicted in Figure 1. Here we consider the case of the single point source for the transmitter, where emitted molecules are diffused through a homogeneous free diffusion medium (3D unbounded without flow), and the receiver is considered as a perfect absorbing sphere of radius r located at a given distance $d > r$ from the transmitter. We consider a binary transmission where the information is encoded in the concentration of molecules. Specifically, the transmission of ones will correspond to the impulsive release of N_{Tx} single-type molecules, zeros will be in correspondence with no emission of molecules as an OOK modulation. The transmission will be periodically triggered with the symbol-period T_{s}.

Considering the emission of N_{Tx} molecules, the fraction of molecules N_{Rx} absorbed by the receiver will be a random quantity because of the randomness of free diffusion media. To account for the N_{Rx} value, three general distributions are reported to model their random behavior as Bernoulli [40], Poisson [5], and Gaussian [33]. These three distributions are dependent on the probability for a single molecule to hit the receiver, defined by the modified inverse Gaussian distribution as [59]

$$p_{\mathrm{hit}}(d,t) = \frac{r(d-r)}{d\sqrt{4\pi D t^3}} e^{-\frac{(d-r)^2}{4Dt}}, \qquad (1)$$

as a time-dependent function in terms of the distance between the transmitter and the receiver $(d-r)$, as well as the diffusion coefficient D (accounting for the physical properties of the medium) as

$$D = \frac{k_{\mathrm{B}}T}{6\pi\eta r_{\mathrm{mol}}}, \qquad (2)$$

where $k_{\mathrm{B}} = 1.38 \cdot 10^{-23}\,\mathrm{J/K}$ is the Boltzman constant, T is the system temperature, η is the medium viscosity,
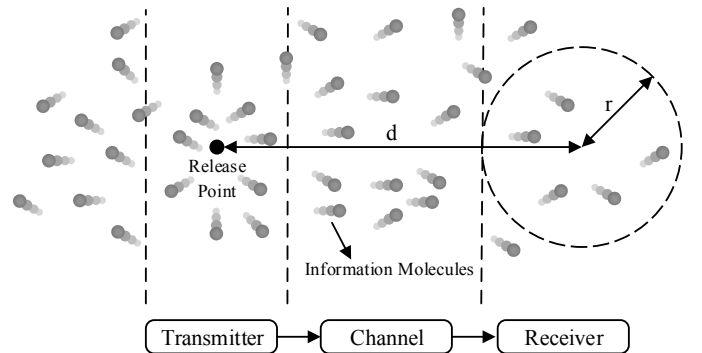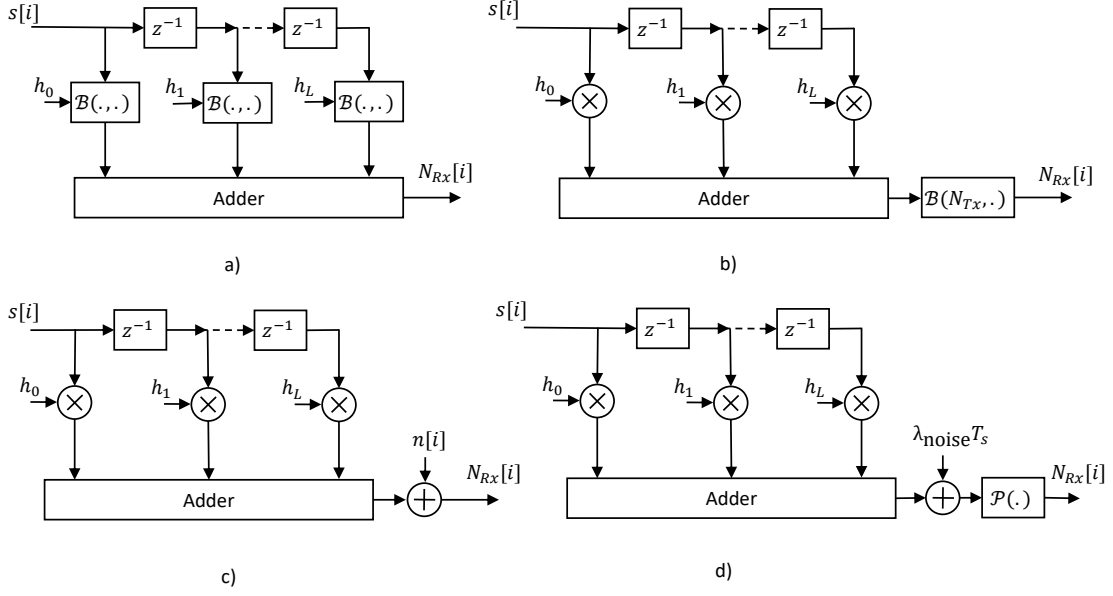

Figure 1: System model.

4

Figure 2: Block diagrams for the MC channel models: (a) Binomial model, (b) approximation of the Binomial model, (c) Normal model, and (d) Poisson model [14].

and r_{mol} represents the radius of the released molecules. Furthermore, the probability of one molecule to reach the destination on a given symbol-time interval (iT_{s}) can be directly computed as

$$
\begin{aligned}
P_i &= \int_{iT_{\mathrm{s}}}^{(i+1)T_{\mathrm{s}}} p_{\mathrm{hit}}(d,t)dt \\
&= \frac{r}{d}\left[\mathrm{erfc}\left(\frac{d-r}{\sqrt{4D(i+1)T_{\mathrm{s}}}}\right) - \mathrm{erfc}\left(\frac{d-r}{\sqrt{4DiT_{\mathrm{s}}}}\right)\right],
\end{aligned}
\tag{3}
$$

where $\mathrm{erfc}(\cdot)$ is the complementary error function.

According to the communication system depicted in Figure 1, the total number of arriving molecules can be modeled by the Bernoulli distribution. That is, when N_{Tx} molecules are released by the transmitter, and considering that any of these molecules have an equal chance to reach the receiver (and only once), then the probability to receive a total of N_{Rx} molecules out of N_{Tx} will follow the binomial distribution as [24]

$$
\begin{aligned}
N_{\mathrm{Rx}}[i] &\sim \mathcal{B}(n_{\mathrm{Rx}}; N_{\mathrm{Tx}}, P_i) \\
&= \binom{N_{\mathrm{Tx}}}{n_{\mathrm{Rx}}} P_i^{n_{\mathrm{Rx}}}(1-P_i)^{N_{\mathrm{Tx}}-n_{\mathrm{Rx}}}.
\end{aligned}
\tag{4}
$$

The relation in Equation (4) only considers the reception of a given transmitted number of molecules, without concerning the impact of ISI produced by previous emissions. To that end, when considering the previous emission of molecules, denoted by the sequence $s[i]$, then the total number of received molecules in the i-th time symbol will be given by the superposition of binomial distributions as

$$
N_{\mathrm{Rx}}[i] \sim \sum_{l=0}^{L} \mathcal{B}(n_{\mathrm{Rx}}; N_{\mathrm{Tx}}s[i-l], P_l),
\tag{5}
$$

where P_l is computed as indicated in Equation (3), and L represents the channel memory length.

To facilitate the analysis, the binomial distribution in Equation (5) is reported to be approximated by the Poisson and Normal distributions to directly compute the total number of received molecules on a given i-th time slot and accounting for ISI. The Poisson distribution is applied under two conditions: arbitrarily large values of the total released molecules (avoiding to specify their exact value), and small probability of each molecules passing through the outlet, yielding [24]

$$
N_{\mathrm{Rx}}[i] \sim \mathcal{P}(\lambda_i) = e^{-\lambda_i}\frac{\lambda_i^{n_{\mathrm{Rx}}}}{n_{\mathrm{Rx}}!},
\tag{6}
$$

where λ_i will be a moderate value [24] defined as [48]

$$
\lambda_i = \lambda_{\mathrm{noise}}T_{\mathrm{s}} + N_{Tx}\sum_{j=0}^{L}s[i-j]P_j,
\tag{7}
$$

λ_{noise} represents an additive stationary noise per unit time due to interfering molecules in the channel (of the same type used to transmit).

On the other hand, the Normal distribution is applied when p_{hit} is sufficiently low yielding [35]

$$
N_{\mathrm{Rx}}[i] \sim \mathcal{N}(\mu_i, \varphi_i^2) = \frac{1}{\sqrt{2\pi}\varphi_i}e^{-\frac{1}{2}\left(\frac{n_{\mathrm{Rx}}-\mu_i}{\varphi_i}\right)^2},
\tag{8}
$$

where

$$\mu_i = N_{\text{Tx}} \sum_{j=0}^{L} s[i-j]P_j, \qquad (9)$$

and

$$\varphi_i^2 = N_{\text{Tx}} \sum_{j=0}^{L} s[i-j]P_j(1-P_j). \qquad (10)$$

Although the natural model for the diffusion process is described by the Binomial distribution, its approximation through Poisson and Normal allows for more mathematical tractability to analyze and design the system. Additionally, the description through the Poisson distribution allows to better model a realistic implementation of transmitters. Typically, there is no control on the exact value regarding the total number of released molecules (N_{Tx}), and the Poisson distribution will "mask" this quantity when expressed in terms of λ instead.

It is also worth mentioning that the mean and variance statistics, regarding these models, are signal-dependent. That is, depending on the transmitted sequence, a larger or reduced impact of ISI will be verified. This concern introduces particular difficulties each time the error probability is part of the system design methodology.

These three different MC channel models can be represented by the block diagrams depicted in Figure 2 [14] for (a) the exact representation of the binomial model, (b) its approximation, (c) the Normal distribution, and (d) the Poisson distribution. In these diagrams, the coefficients h_i represent the probability to receive a molecule in a given time slot i as P_i in Equation (3). By means of these filter-approach models, it is possible to simulate the received concentration with reduced computational complexity.

3.2. K-bit MC Receiver

Several receiver schemes have been reported to account for a reduced impact regarding ISI. In the case of binary transmissions, the reported schemes decode the received sequence by directly comparing the sampled concentration of molecules to a threshold value τ in order to decide whether a 0 or a 1 was transmitted. The value of τ is optimally computed to minimize the BER metric [48].

These threshold-based detectors are mainly distinguished by their accuracy in estimating the value of τ. For instance, the zero-bit memory receiver will establish τ based on the current symbol, while a K-bit memory receiver will also use the previous K symbols to compute the optimal threshold value. Assuming a Poisson channel model, a K-bit memory receiver will implement an optimal threshold computed as [48]

$$\tau^*[i] = \arg\min_{\tau} P_e(\tau, i), \qquad (11)$$

where

$$P_e(\tau, i) = \frac{1}{2^{L-K}} \sum_{k=i-K+1}^{i-1} P_e(s[k], \tau), \qquad (12)$$

is the error probability, and

$$P_e(s[k], \tau) = \frac{1}{2} \Bigg[Q\left(\lambda_0 T_{\text{s}} + \sum_{j=1}^{L} s[k-j]C_j, \lceil \tau \rceil \right) + 1 -$$

$$- Q\left(\lambda_0 T_{\text{s}} + \sum_{j=1}^{L} s[k-j]C_j + C_0, \lceil \tau \rceil \right) \Bigg], \qquad (13)$$

where $Q(\lambda, n) = \sum_{k=n}^{\infty} \frac{e^{-\lambda}\lambda^k}{k!}$ is the incomplete Gamma function, λ_0 is the background noise per unit time, the term

$$C_j = N_{\text{Tx}}P_j \qquad (14)$$

denotes the average received total number of particles at the j-th slot produced by one particular emission of N_{Tx} molecules, and P_j is the probability that one molecule hits the receiver at the given time slot according to Equation (3).

The noisy contribution of ISI, considered by the $s_{i-j}C_j$ and C_0 terms for the error probability in Equation (13), will be dependent on the transmitted sequence vector $s[i]$. The larger the total number of previous symbols with high concentration, the larger the contribution of ISI to the current symbol will be. In general, the error probability value P_e will be also a random variable.

3.3. AoI Metrics

A natural definition to account for the age of given information carried by a packet is given by the time elapsed since its creation. Considering that a given packet was created in the time instant t_p, then its corresponding age will be given by $\Delta_p(t) = t - t_p$, as depicted by dashed lines in Figure 3 [58], where five packets are represented and periodically created in the time instants t_1 to t_5. Considering the destination node, let us assume all these packets arrive successfully but for the third one because of the produced errors by the channel noise. The successful packet's arrival will update the status and correspondingly the perceived AoI. In correspondence, the current AoI regarding the source's status will be given by the age of the most recent packet received at the destination node as depicted
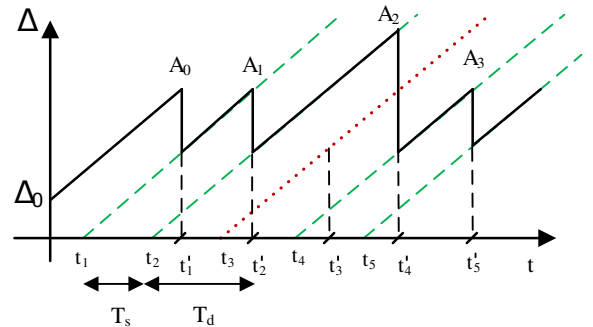

Figure 3: Representation of the AoI of packets (dashed lines) and as perceived on a given destination node (bold line).

by the solid line in Figure 3. According to this definition, the AoI will be given by a piece-wise function, where each segment will be defined by

$$\Delta(t) = t - u(t), \tag{15}$$

and $u(t)$ corresponds to the time-stamp of the most recent received packet. Due to the randomness of transmissions (produced by channel impairments and the communication network mechanisms), packets will arrive randomly, which in turn will imply that $u(t)$ will be a random process, and subsequently the AoI as well.

Considering the AoI random process in Equation (15), several metrics are defined to optimize the freshness of information on the received side. The time-average AoI, computed as

$$\langle \Delta \rangle = \lim_{T \to \infty} \frac{1}{T} \int_0^T \Delta(t) dt, \tag{16}$$

will account for the area under the piece-wise function $\Delta(t)$. On the other hand, the PAoI will average the peaks A_n (local maximums) regarding the AoI curve in Figure 3 yielding

$$\Delta^{(p)} = \lim_{T \to \infty} \frac{1}{N(T)} \sum_{n=1}^{N(T)} A_n, \tag{17}$$

where $N(T)$ represents the total number of peaks up to T. This metric is more tractable analytically than the average AoI because of their linear relation to time intervals. As depicted in Figure 3, it will be given by a linear superposition of non-overlapping time intervals as $A_n = Y_n + T_n$, where Y_n is the time-period of transmissions, and T_n is the time elapsed since the packet transmission to their reception.

These AoI metrics provide a means to improve the freshness of the status updates about a remote sensor considering the restriction imposed by the communication system. Focusing particularly on the MC scenario, as depicted in Figure 1, the MC channel will introduce two main restrictions to achieve timely updated packets: the propagation delay through the medium (by means of free diffusion), and the errors introduced by the impact of ISI. These undesirable channel effects must be properly considered to obtain a reduced AoI metric.

When attempting to improve the freshness of the status update, there will be a trade-off mechanism between an increased rate of transmission and the channel effect. To illustrate, let us consider to increase the rate of transmission. Accordingly, this will be in favor of an increasing rate of packet arrivals (and consequently a reduced latency), but also a non-desirable increased rate of packet dropping because of the impact of ISI, which in turn will degrade the status about the source update. In this regard, the AoI metrics will account for this balance provided it will jointly capture the rate of emissions and the impact of delay and errors produced by the channel. These metrics will allow deriving the optimal rate of transmission to have updates as fresh as possible.
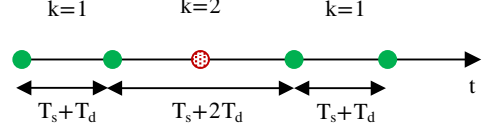

Figure 4: Illustration how to compute the average PAoI.

3.4. Average PAoI for MC Channels

We now compute the average PAoI metric regarding the system model depicted in Figure 1. We will assume that packets are transmitted periodically with the time symbol T_s (deterministic) through a time-invariant channel with constant propagation delay T_d. We assume that the propagation delay will be given by the time according to the maximum probability for a molecule to impact the receiver (pulse peak time [59]), i.e., when $p_{hit}(d, t)$ in Equation (1) is maximum, yielding

$$T_d = \frac{(d - r)^2}{6D}. \tag{18}$$

The value of T_d becomes certain when considering the emission of large number of molecules. Following the solution to the Fick's second law, the received concentration-peak will be perceived after T_d seconds as given in Equation (18) [13]. Additionally, we assume a perfectly synchronized system, where the receiver will sample the concentration of molecules on each symbol time-interval according to $t_k = kT_s + T_d$, where $k \in \{0, 1, 2, \dots\}$.

When received, packets may be corrupted due to the noise and interference in the channel. In such a case, the information concerning this packet is discarded as it does not provide a meaningful status about the source. When two consecutive packets arrive successfully, then their corresponding PAoI will be directly given by a deterministic quantity as $A_i = T_s + T_d$. However, when the second packet is corrupted but the third one is successfully received, then their corresponding peak will be given by $A_i = T_s + 2T_d$, as depicted in Figure 4. In general, when the next $(k - 1)$ packets are corrupted but the k-th is successfully received, then

$$A_n = T_s + kT_d, \tag{19}$$

for $k > 0$. Furthermore, provided that errors will occur randomly, then A_n will be a random variable regarding the natural integer $k > 0$. That is, the value of $k = 1$ will correspond to two consecutive packets successfully received, $k = 2$ to the case of not the second but to the third one successfully received, and so on. By this approach, the average PAoI will be given after obtaining the average of the random variable k as

$$\Delta^{(p)} = \mathbb{E}[A_n] = T_s + \mathbb{E}[k]T_d. \tag{20}$$

The value of $\mathbb{E}[k]$ in Equation (20) can be computed by recalling the negative binomial distribution as follows [24]. Taking into account a succession of n Bernoulli trials, assuming equal probability of successful packet detection

7

$p_d = 1 - p_e$, then the probability that the r-th success occurs at a given trial number $(r + l)$ can be evaluated through the negative binomial distribution as [24]

$$f(l; r, p_d) = \binom{-r}{l} p_d^r (p_d - 1)^l. \tag{21}$$

with the expected value

$$\mathbb{E}[l] = \sum_{l=0}^{\infty} l \binom{-r}{l} p_d^r (p_d - 1)^l = r \frac{1 - p_d}{p_d}. \tag{22}$$

By using this distribution, we can compute the corresponding expected value for k assuming a constant value of p_d. Although p_d will be dependent on the transmitted sequence, as discussed in Section 3.2, we can consider the worst-case scenario for the larger ISI (all the previous symbols with the larger concentration), or consider the mean value of the transmitted sequence $s[i]$, which is constant for stationary sources.

To evaluate the expected value for k, we depart from a packet successfully received considering that k represents the gap size between two successfully received packets, as depicted in Figure 4. Then, the probability to find the next successfully packet, at any arbitrary index k, can be obtained by evaluating Equation (21) for $r = 1$ (next first success) at the trial number $(r+l)|_{l=k-1}$. Then, considering the formula for the expected value of the distribution in Equation (22) and considering that $k = l + 1$, the expected value for k will be given as

$$\mathbb{E}[k] = 1 + \frac{1 - p_d}{p_d}. \tag{23}$$

Finally, after replacing Equation (23) in Equation (20), we obtain the desired formula for the average PAoI as

$$\Delta^{(p)} = \mathbb{E}[A_n] = T_s + \frac{1}{p_d} T_d, \tag{24}$$

or equivalently, in terms of the error probability (p_e), as

$$\Delta^{(p)} = \mathbb{E}[A_n] = T_s + \frac{1}{1 - p_e} T_d, \tag{25}$$

Considering the derived relation in Equation (25), a system with a perfect packet reception ($p_e = 0$) will exhibit a minimum age corresponding to $(T_s + T_d)$ in accordance to a preliminary ideal system overview, i.e., in the absence of errors, when a packet arrives, then the previously received packet will be already aged by the time elapsed in between both (given by T_s) plus the propagation delay (T_d). On the other hand, considering the impact of errors, the relation in Equation (25) will exhibit a counteract-mechanism when trying to reduce the expected PAoI by reducing the time symbol value T_s. When the value of T_s is reduced, the first term in Equation (25) is correspondingly diminished (the desired effect), but the p_e value will be increased as well due to the impact of ISI, and thus the second term will be increased (non-desired effect).
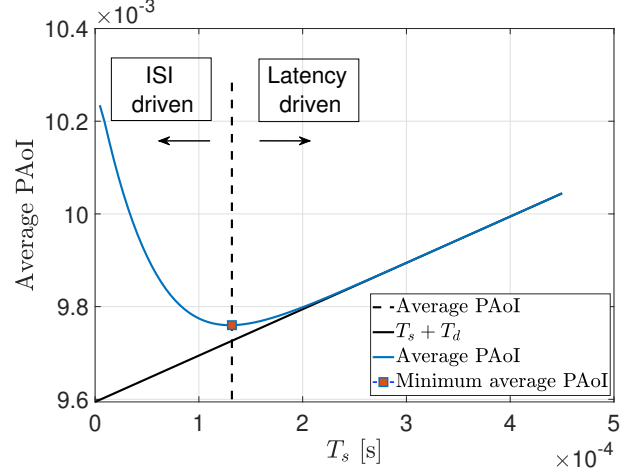

Figure 5: Average PAoI.

This trade-off between the rate of transmission and performance, jointly captured by the AoI metric, can be optimally solved when stating an optimal problem formulation. This topic will be further discussed in the following.

3.5. Optimal Transmission Rate for Minimal Average PAoI

Considering the computed average PAoI (cf. Equation (20)), the optimal trade-off between a reduced symbol time T_s and the counteract mechanism of increased p_e can be stated as (assuming that p_e is time-independent)

$$\Delta_{\min}^{(p)} = \min_{T_s} T_s + \frac{1}{1 - p_e(T_s)} T_d, \tag{26}$$

where the relation between p_e and T_s have been declared explicitly. That is, $\Delta_{\min}^{(p)}$ will provide the minimum achievable PAoI after optimally determining T_s.

Based on a K-bit memory receiver implementation, a closed-form expression as a solution to the optimization problem formulation in Equation (26) cannot be derived. The variable T_s is not only a linear term but also the argument of an exponential function, as expressed by the incomplete gamma function for the relation in Equation (13) when evaluating the error probability term. Instead, the solution to Equation (26) must be solved numerically.

As an illustration, Figure 5 depicts the objective function for the zero-bit memory receiver using the system parameters described in Table 1. The threshold is approximated as [48]

$$\tau = \frac{C_0}{\ln \left(1 + \frac{C_0}{\sum_{i=1}^{L} \frac{C_i}{2} + \lambda_0 T_s}\right)}, \tag{27}$$

for the worst-case scenario when the transmitted sequence is given by all ones as $s_i = 1$, and the coefficients C_i are computed as indicated in Equation (14). The error probability is computed as described in Equation (12) for $K = 0$, after replacing the value of τ in Equation (13).

8

Parameter	Value
Diffusion coefficient D	$426.5\,\mu\text{m}^2/\text{s}$
Background noise per unit time λ_0	$100\,\text{s}^{-1}$
Distance d	$5\,\mu\text{m}$
Receiver radius r	$45\,\text{nm}$
Channel length L	5

Table 1: System parameters (derived from [48]).

In this specific example, here we consider the emission of binary symbols, thus packets will be comprised by one-bit only. Additionally, we have considered the worst-case scenario for the larger ISI

The curve in Figure 5 depicts a concave function of the time symbol (T_s) as a result of evaluating the objective function in Equation (26) by using the parameters in Table 1. It becomes apparent that the last term in Equation (25) will be dominant for small values of T_s, where the impact of errors will introduce the larger age. For larger values of T_s, the average PAoI will asymptotically behave as ($T_s + T_d$), where the impact of latency will produce the increased age. In between these two asymptotic behaviors, the minimum average PAoI will be located, which in turn will provide the optimum balance to account for a timely updated system. Here we consider that latency is introduced by the propagation delay plus the time it takes to send a new symbol through T_s, the delay introduced for decoding is assumed negligible considering the reception of binary symbols.

4. Simulation Results

In this section, we illustrate the agreement between the theoretical formulation and simulation results. We also evaluate the impact of the varying propagation distance between the transmitter and the receiver, the radius of the receiver, and the diffusion coefficient as well. Regarding the theoretical formulation, we solve the problem formulation in Equation (26) numerically by an exhaustive search plan.

Simulation results are derived for a total number of 10^4 transmitted symbols when implementing the system model represented in Figure 2 d). Then, after comparing the output sequence with the threshold level in Equation (27), we estimate the transmitted sequence of ones and zeros. We determine the errors by directly comparing the estimated sequence with the transmitted one. The error detection is then used to compute the average PAoI to illustrate the numerical evaluation. Theoretical and simulation results are derived for the parameters given in Table 1.

We evaluate the PAoI sequence A_n in Equation (15) after properly obtaining the value of k as follows: Whenever an error is detected, the value of k is increased, otherwise $k = 1$. Then, the average PAoI is computed by averaging the obtained sequence of peaks. The results are shown in Figure 6, where the theoretical formula derived in Equation (25) agrees with the simulated curve. The figure also
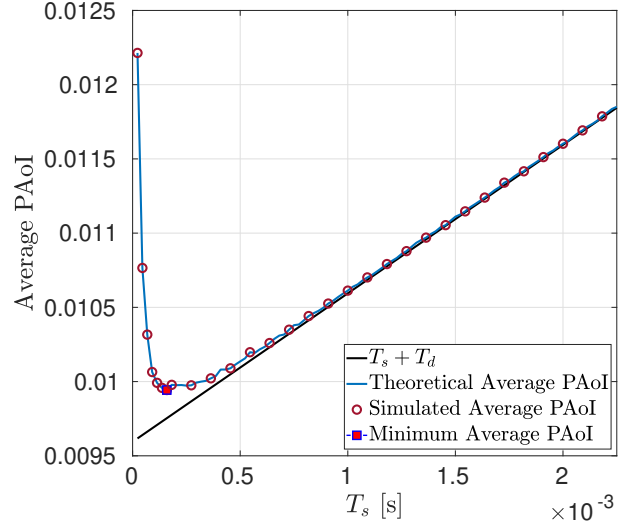

Figure 6: Simulated and theoretical average PAoI when the receiver radius is $r = 45\,\text{nm}$, the propagation distance is $d = 5\,\mu\text{m}$, and the diffusion coefficient is $D = 426.5\,\mu\text{m}^2/\text{s}$.
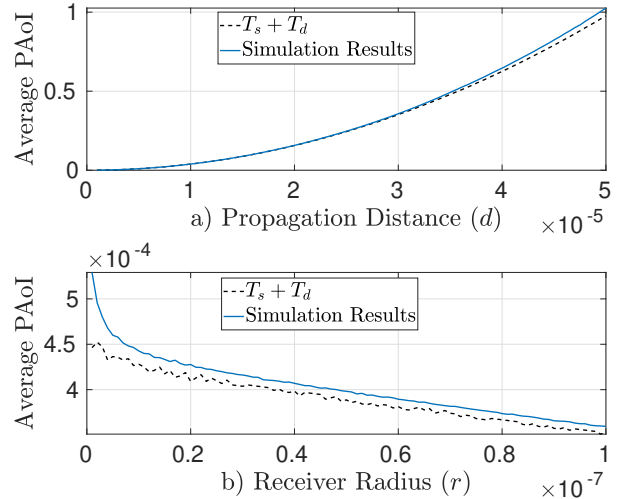

Figure 7: Average PAoI for a) varying propagation distance when the receiver radius is $r = 45\,\text{nm}$, and b) for a varying receiver radius when $d = 5\,\mu\text{m}$. The diffusion coefficient is $D = 426.5\,\mu\text{m}^2/\text{s}$.

exhibits the trade-off between the produced errors by ISI (due to a reduced symbol time) and the increased information age because of the increased latency. The local minimum will provide the optimal selection regarding the value of T_s to implement a system as fresh as possible.

Figure 7 shows the simulation results accounting for a varying distance and received radius in a) and b), respectively. The minimum average PAoI is decremented whenever the propagation distance is reduced or the receiver radius is increased. The less the propagation distance or the greater the receiver radius, the lower are the errors in detecting the transmitted symbols due to an increased

concentration of molecules on the receiver side. This, in turn, will imply a reduction in the average PAoI to get close to the optimal performance (depicted with dotted lines).

However, considering the curves in Figure 7 the resulting impact in the average PAoI will be more noticeable regarding the variation of r than d. To provide a metric regarding the impact of d and r in the resulting average PAoI, we consider the mean curvature of both curves in Figure 7. We compute numerically the curvature as $\bar{k} = \frac{1}{b-a}\int_a^b k(x)\mathrm{d}x$, where $k(x) = \frac{f''(x)}{(1+f'^2(x))^{3/2}}$, and $f(x)$ represents the given curve. Considering that the curvature will measure the amount of which $f(x)$ will deviate from a straight line, it will provide a metric of variability of $f(x)$ with the variation of x. The larger the mean curvature, the larger the impact of the independent variable x regarding $f(x)$ will be.

By this procedure, the mean curvature of the average PAoI is $4.834 \ 10^{-6}$ and $6.078 \ 10^{-5}$ for the propagation distance d and the receiver radius r, respectively. That is, by this metric the impact of the receiver radius will be higher than the propagation distance (ten times larger). The freshness of the system is more rapidly improved by varying the receiver radius than by varying the propagation distance.

Figure 8 a) depicts the numerical solution for the optimal symbol time T_{s} regarding a varying propagation distance d and Figure 8 b) shows the results for a varying receiver radius r. To have an optimally fresh system in favor of the best balance between the impact of ISI and latency, the value of T_{s} must be increased with d and decreased with r. The optimum solution for the varying propagation distance (graph in a)) exhibits an exponential behavior as $ae^{b \cdot d}$, where $a = 8.6 \cdot 10^{-5}$, $b = 9.7 \cdot 10^4$, with a root mean square error equals to $2.3 \ 10^{-4}$. On the other hand, the optimal solution for the varying receiver radius (graph in b)) follows a two-terms exponential function as $\sum_{i=1}^{2} a_i e^{b_i \cdot d}$, where $a_1 = 3.1 \cdot 10^{-4}$, $a_2 = 1 \cdot 10^{-4}$, $b_1 = -6.9 \cdot 10^7$, and $b_2 = -1.8 \cdot 10^{-6}$, with a root mean square error equal to $1.6 \ 10^{-5}$.

To illustrate the impact of the molecule interactions with the propagation medium, Figure 9 depicts the obtained average PAoI regarding a few diffusion coefficients. A higher diffusion coefficient will imply that the given particle will displace larger distances due to its reduced size (assuming a constant viscosity and system temperature) in favor of the timely system update. For instance, insulin in water ($D = 150 \, \mu\mathrm{m}^2/\mathrm{s}$) will exhibit a lower average PAoI than a bigger particle like albumin in water ($D = 69 \, \mu\mathrm{m}^2/\mathrm{s}^3$) or even bigger like a magnetic particle ($D = 4.53 \, \mu\mathrm{m}^2/\mathrm{s}$) [55].

---

[3]Search BioNumbers – The Database of Useful Biological Numbers, `https://bionumbers.hms.harvard.edu/search.aspx`
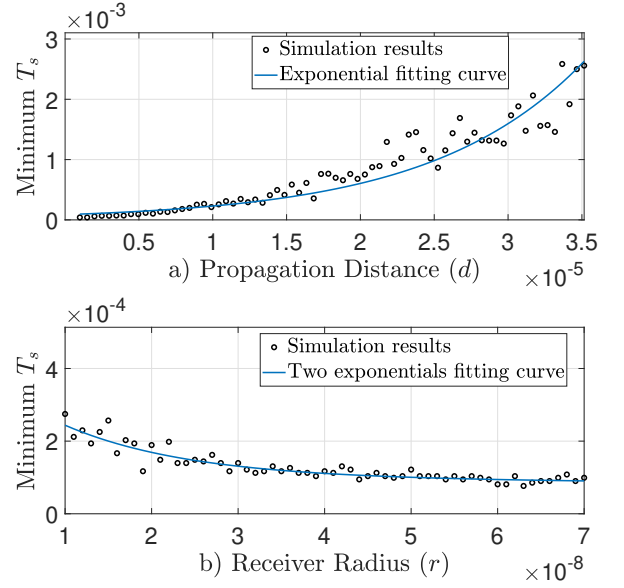

Figure 8: Optimal symbol-period T_{s} for a) varying propagation distance when the receiver radius is $r = 45\,\mathrm{nm}$, and b) for a varying receiver radius when $d = 5\,\mu\mathrm{m}$. The diffusion coefficient is $D = 426.5\,\mu\mathrm{m}^2/\mathrm{s}$.

5. Open Research Issues

Considering the concept of AoI and its corresponding metrics to account for the system status updates, its application to MC will identify a variety of open directions. Some research topics can be defined in parallel to the reported conventional electromagnetism-based systems, some others can be newly stated regarding the specifics of MC communication systems. In this section we summarize some open problems with relevance to future research relying on
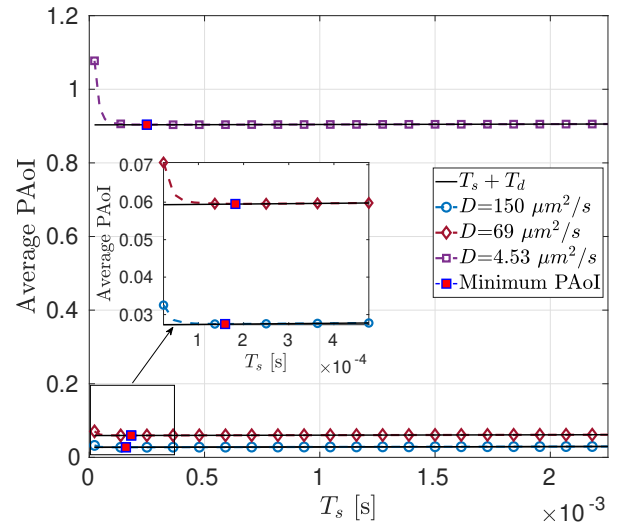

Figure 9: Average PAoI with varying diffusion coefficient when $d = 5\,\mu\mathrm{m}$ and $r = 45\,\mathrm{nm}$.

the AoI concept.

5.1. Accurately Computing the AoI

The average PAoI metric – as derived in Equation (25) – assumes that the errors produced by the impact of ISI are independent regarding the transmitted sequence status. Although it is valuable to study the impact of worst-case scenarios or the average system behavior, their accurate derivation is still to be obtained. In this direction, the Stochastic Hybrid System (SHS) [57] approach could be used to compute the AoI metrics, where the corresponding Markov-chain transition probabilities may account for the sequence transmission status.

5.2. System Utilization

To provide a metric regarding the system utilization, the ratio between the transmission and server rates must be computed. Considering the system model described in this paper, where the given MC system is not comprised by queues, the reception, and transmission of packets will be deterministically handled and the rate of service will be upper-bounded by the equivalent system bandwidth. In this case, the randomness will be given by the discarded packets due to errors produced in the MC channels. The equivalent system bandwidth can be derived by considering the reported models in [45, 12], where the channel response, as well as the transmitter and receiver implementations, are jointly addressed. However, when considering channels with memory, where the channel response will be dependent on previous emissions (i.e., modeled by the channel coefficients h_i in Figure 2), then the rate of transmission will become part of the computation.

5.3. Transmission Medium

In addition to the free-diffusion medium, several other mechanisms have been reported to provide communication means. Self-powered systems like molecular-motor, diffusion with the flow, microfluidic MC, and reaction channels are examples of the variety of supporting communication mechanisms in addition to the simple case of free-diffusion [35]. These different MC channels will introduce their own restrictions and particularities that will impact the communication performance. For instance, in the reaction channels, the emitted molecules may be degraded because they will chemically react with other molecules in the channel [12], which in turn will imply a reduced total number of molecules and additional noise in the channel. The dynamic of such mechanisms will impact the aging regarding the status updates. As another example, in flow-based systems such as the cardio vascular system, the flow dynamics will further impact the transmission dynamics [16]. The evaluation of the MC metrics accounts for the optimal use of the available communication resources regarding these different communication channels.

5.4. Information-Theoretic Approach

AoI and mutual information are linked concepts to account for "information aging" [53]. By this approach, the freshness of received samples will be given by the information they carry about current emissions in the source. Analytically, a given received sample will be aged as long as its conditional entropy (regarding the emitted symbol) increases, i.e., the received packet is less able to predict emissions on the source. Considering the body of works already reported for the derived mutual information in MC channels [4, 26], their extension to analyze information aging through the lens of the AoI concept can also be handled.

5.5. Dissemination of the CSI

Typically, the receiver settings to optimize performance depend on the previous knowledge about the channel state information (CSI). For instance, the threshold level can be optimally settled to avoid the impact of ISI when implementing sampling-based detectors [36]. Considering the highly time-varying behavior of MC channels, timely updates about the channel condition will be of major importance to implement optimal receivers, and minimum-aged information systems. The obtaining of AoI metrics concerning the CSI status and their impact on the system performance would help to provide further insights.

5.6. Mobile Environments

Mobile environments are considered for non-static positions regarding the transmitter and the receiver. To account for the optimal reception in such a dynamic environment, some reported solutions reconstruct the CSI on each symbol interval [1, 11] or they implement an adaptive threshold mechanism to adjust the system parameters dynamically [50]. The impact of the movement of nodes in the rate of updates regarding the dynamics of movement can be analyzed from the perspective of the AoI concept.

5.7. Feedback Channels

Feedback channels are typically employed as a flow control mechanism to dynamically regulate the transmission rate and avoid buffer saturation, for instance, [42]. Besides, in some applications, when packets are received with errors, those must be retransmitted under some policies by implementing a feedback mechanism to the source. The delay introduced by feedback channels and their reliability should be considered when minimizing the AoI.

5.8. Thermodynamic Limits

Considering MC and living cells as communication systems, there is a thermodynamic limit regarding the unit of information represented by the communication scheme [7]. Inherently, the constituting elements of MC systems will establish a lower bound on the energy-per-bit to establish communication at a given distance and with the specifics of the MC channels [2, 18]. Additionally, considering that

AoI and information are connected concepts, a theoretical study concerning the thermodynamic of the represented unit of information can be extended to the thermodynamic limit to achieve a certain level regarding the freshness of information.

5.9. System Complexity

Because of the reduced available resources of nanomachine devices, it is imperative to implement systems of reduced complexity [35]. For instance, the mechanisms to protect data against the channel noise (error-correcting codes) must be as simple as possible. However, such reduced complex mechanisms will be less robust to the MC channel effects, which in turn will imply a degraded reception process, and consequently a resulting increase of the AoI metric. A proper balance between the system complexity and robustness can be achieved by means of the AoI metrics. In addition, the achievable bounds regarding the freshness of status updates in terms of the complexity of such mechanisms can be analyzed as well.

5.10. Simulation Environments

Simulation environments will account for more realistic scenarios than those considered by the theoretical formulation. For instance, sedimentation, geometry, or obstacles can be effectively included to account for a realistic communication link. Better modeling, regarding the AoI evolution, can be derived to compute corresponding metrics supported by the simulation environment. In addition, the AoI metrics can also be included in the resulting performance for the simulation environment to account for the freshness of the given systems. Specifically, when accounting for MC-networks, the simulation tools can overcome the theoretical complexity when computing their corresponding AoI metric.

6. Conclusion

Information aging concepts are required for the design of timely updated communication systems. In this regard, the use of age of information (AoI) metrics plays a major role. For the first time, we introduce the concept of AoI for analyzing and designing the status update in nanonetworks, where nanodevices cooperate by exchanging data over molecular communication (MC) channels. We have introduced this concept to reveal the counter-acting mechanism when implementing an optimally fresh MC channel. We particularly focused on the peak age of information (PAoI), which describes the maximum AoI on a per-packet basis. The resulting trade-off between latency and ISI helps studying the optimal solution for the system utilization. We also validated the derived analytical expressions by means of simulation. Although considered for a point-to-point connection, this first approach can be further extended to multi-hop nanonetworks to optimize their performance regarding fresh status updates. In this direction, we outlined several open research problems that need to be addressed to further apply the AoI concept.

Acknowledgments

References

[1] Arman Ahmadzadeh, Vahid Jamali, and Robert Schober. 2018. Stochastic Channel Modeling for Diffusive Mobile Molecular Communication Systems. *IEEE Transactions on Communications* (Dec. 2018), 6205 – 6220. `https://doi.org/10.1109/TCOMM.2018.2854577`

[2] Ozgur B. Akan, Hamideh Ramezani, Tooba Khan, Naveed A. Abbasi, and Murat Kuscu. 2017. Fundamentals of Molecular Information and Communication Science. *Proc. IEEE* 105, 2 (Feb. 2017), 306–318. `https://doi.org/10.1109/jproc.2016.2537306`

[3] Ian F. Akyildiz, Faramarz Fekri, Raghupathy Sivakumar, Craig R Forest, and Brian K Hammer. 2012. Monaco: fundamentals of molecular nano-communication networks. *IEEE Wireless Communications* 19, 5 (2012), 12–18. `https://doi.org/10.1109/MWC.2012.6339467`

[4] Ian F. Akyildiz, Massimiliano Pierobon, and Sasitharan Balasubramaniam. 2019. An Information Theoretic Framework to Analyze Molecular Communication Systems Based on Statistical Mechanics. *Proc. IEEE* 107, 7 (July 2019), 1230 – 1255. `https://doi.org/10.1109/JPROC.2019.2927926`

[5] Hamidreza Arjmandi, Amin Gohari, Masoumeh Nasiri Kenari, and Farshid Bateni. 2013. Diffusion-Based Nanonetworking: A New Modulation Technique and Performance Analysis. *IEEE Communications Letters* (March 2013), 645 – 648. `https://doi.org/10.1109/LCOMM.2013.021913.122402`

[6] Michael Taynnan Barros, Sasitharan Balasubramaniam, Brendan Jennings, and Yevgeni Koucheryavy. 2014. Transmission Protocols for Calcium-Signaling-Based Molecular Communications in Deformable Cellular Tissue. *IEEE Transactions on Nanotechnology* 13, 4 (July 2014), 779–788. `https://doi.org/10.1109/tnano.2014.2321492`

[7] Charles H. Bennett. 1988. Notes on the history of reversible computation. *IBM Journal of Research and Development* 32, 1 (Jan. 1988), 16–23. `https://doi.org/10.1147/rd.321.0016`

[8] Howard C. Berg. 1993. *Random Walks in Biology*. Princeton University Press.

[9] Fabian Bronner and Falko Dressler. 2019. Towards Mastering Complex Particle Movement and Tracking in Molecular Communication Simulation. In *6th ACM International Conference on Nanoscale Computing and Communication (NANOCOM 2019), Poster Session*. ACM, Dublin, Ireland, 36:1–36:2. `https://doi.org/10.1145/3345312.3345490`

[10] Yesenia Cevallos, Luis Tello-Oquendo, Deysi Inca, Debasish Ghose, Amin Zadeh Shirazi, and Guillermo A. Gomez. 2019. Health Applications Based on Molecular Communications: A Brief Review. In *IEEE International Conference on E-health Networking, Application & Services (HealthCom 2019)*. IEEE, Bogotá, Colombia. `https://doi.org/10.1109/healthcom46333.2019.9009607`

[11] Ge Chang, Lin Lin, and Hao Yan. 2018. Adaptive Detection and ISI Mitigation for Mobile Molecular Communication. *IEEE Transactions on NanoBioscience* 17, 1 (Jan. 2018), 21–35. `https://doi.org/10.1109/tnb.2017.2786229`

[12] Chun Tung Chou. 2013. Extended Master Equation Models for Molecular Communication Networks. *IEEE Transactions on NanoBioscience* 12, 2 (June 2013), 79–92. `https://doi.org/10.1109/tnb.2013.2237785`

[13] John Crank. 1986. *The Mathematics Of Diffusion* (2 ed.). Oxford University Press.

[14] Martin Damrath, Sebastian Korte, and Peter Adam Hoeher. 2017. Equivalent Discrete-Time Channel Modeling for Molecular Communication With Emphasize on an Absorbing Receiver. *IEEE Transactions on NanoBioscience* 16, 1 (Jan. 2017), 60–68. `https://doi.org/10.1109/tnb.2017.2648042`

[15] Martin Damrath, Jerin Joseph Koshy, and Peter Adam Hoeher. 2017. Application of OFDM in Diffusion-Based Molecular Communication. *IEEE Transactions on Molecular, Biological and Multi-Scale Communications* 3, 4 (Dec. 2017), 254–258. `https://doi.org/10.1109/tmbmc.2018.2886833`

[16] Jan Peter Drees, Lukas Stratmann, Fabian Bronner, Max Bartunik, Jens Kirchner, Harald Unterweger, and Falko Dressler. 2020. Efficient Simulation of Macroscopic Molecular Communication: The Pogona Simulator. In *7th ACM International Conference on Nanoscale Computing and Communication (NANOCOM 2020)*. ACM, Virtual Conference. `https://doi.org/10.1145/3411295.3411297`

[17] Andrew W. Eckford. 2007. Nanoscale Communication with Brownian Motion. In *41st Annual Conference on Information Sciences and Systems (CISS 2007)*. IEEE, Baltimore, MD. `https://doi.org/10.1109/ciss.2007.4298292`

[18] Andrew W. Eckford, Benjamin Kuznets-Speck, Michael Hinczewski, and Peter J. Thomas. 2018. Thermodynamic Properties of Molecular Communication. In *IEEE International Symposium on Information Theory (ISIT 2018)*. IEEE, Vail, CO. `https://doi.org/10.1109/isit.2018.8437793`

[19] Nariman Farsad, Weisi Guo, and Andrew W. Eckford. 2013. Tabletop Molecular Communication: Text Messages through Chemical Signals. *PLOS ONE* 8, 12 (Dec. 2013), 1–13. `https://doi.org/10.1371/journal.pone.0082935`

[20] Nariman Farsad, David Pan, and Andrea Goldsmith. 2017. A Novel Experimental Platform for In-Vessel Multi-Chemical Molecular Communications. In *IEEE Global Communications Conference (GLOBECOM 2017)*. IEEE, Singapore, Singapore. `https://doi.org/10.1109/glocom.2017.8255058`

[21] Nariman Farsad, H. Birkan Yilmaz, Andrew W. Eckford, Chan-Byoung Chae, and Weisi Guo. 2016. A Comprehensive Survey of Recent Advancements in Molecular Communication. *IEEE Communications Surveys & Tutorials* 18, 3 (2016), 1887–1919. `https://doi.org/10.1109/comst.2016.2527741`

[22] Luca Felicetti, Mauro Femminella, and Gianluca Reali. 2013. Simulation of molecular signaling in blood vessels: Software design and application to atherogenesis. *Elsevier Nano Communication Networks* 4, 3 (Sept. 2013), 98–119. `https://doi.org/10.1016/j.nancom.2013.06.002`

[23] L. Felicetti, M. Femminella, G. Reali, and P. Liò. 2016. Applications of molecular communications to medicine: A survey. *Nano Communication Networks* 7 (March 2016), 27–45. `https://doi.org/10.1016/j.nancom.2015.08.004`

[24] William Feller. 1968. *An Introduction to Probability Theory and Its Applications* (3 ed.). Vol. 1. Wiley.

[25] Nora Garralda, Ignacio Llatser, Albert Cabellos-Aparicio, Eduard Alarcón, and Massimiliano Pierobon. 2011. Diffusion-based physical channel identification in molecular nanonetworks. *Nano Communication Networks* 2, 4 (Dec. 2011), 196–204. `https://doi.org/10.1016/j.nancom.2011.07.001`

[26] A. Gohari, M. Mirmohseni, and M. Nasiri-Kenari. 2016. Information theory of molecular communication: directions and challenges. *IEEE Transactions on Molecular, Biological and Multi-Scale Communications (T-MBMC)* 2, 2 (Dec. 2016), 120–142. `https://doi.org/10.1109/TMBMC.2016.2640284`

[27] W. Guo, C. Mias, N. Farsad, and J. Wu. 2015. Molecular Versus Electromagnetic Wave Propagation Loss in Macro-Scale Environments. *IEEE Transactions on Molecular, Biological and Multi-Scale Communications (T-MBMC)* 1, 1 (March 2015), 18–25. `https://doi.org/10.1109/TMBMC.2015.2465517`

[28] Werner Haselmayr, Andreas Springer, Georg Fischer, Christoph Alexiou, Holger Boche, Peter Adam Hoeher, Falko Dressler, and Robert Schober. 2019. Integration of Molecular Communications into Future Generation Wireless Networks. In *1st 6G Wireless Summit*. IEEE, Levi, Finland.

[29] Vahid Jamali, Arman Ahmadzadeh, Wayan Wicke, Adam Noel, and Robert Schober. 2019. Channel Modeling for Diffusive Molecular Communication—A Tutorial Review. *Proc. IEEE* 107, 7 (July 2019), 1256–1301. `https://doi.org/10.1109/jproc.2019.2919455`

[30] Yubing Jian, Bhuvana Krishnaswamy, Caitlin M. Austin, A. Ozan Bicen, Jorge E. Perdomo, Sagar C. Patel, Ian F. Akyildiz, Craig R. Forest, and Raghupathy Sivakumar. 2016. nanoNS3: Simulating Bacterial Molecular Communication Based Nanonetworks in Network Simulator 3. In *3rd ACM International Conference on Nanoscale Computing and Communication (NANOCOM 2016)*. ACM, New York City, NY, 17:1–17:7. `https://doi.org/10.1145/2967446.2967464`

[31] B. H. Koo, C. Lee, H. Birkan Yilmaz, N. Farsad, Andrew W. Eckford, and C. B. Chae. 2016. Molecular MIMO: From Theory to Prototype. *IEEE Journal on Selected Areas in Communications (JSAC)* 34, 3 (March 2016), 600–614. `https://doi.org/10.1109/JSAC.2016.2525538`

[32] Mehmet Sukru Kuran, H. Birkan Yilmaz, Ilker Demirkol, Nariman Farsad, and Andrea Goldsmith. 2021. A Survey on Modulation Techniques in Molecular Communication via Diffusion. *IEEE Communications Surveys & Tutorials* 23, 1 (Jan. 2021), 7–28. `https://doi.org/10.1109/comst.2020.3048099`

[33] Mehmet Şükrü Kuran, H. Birkan Yilmaz, Tuna Tugcu, and Ian F. Akyildiz. 2011. Modulation Techniques for Communication via Diffusion in Nanonetworks. In *IEEE International Conference on Communications (ICC 2011)*. Kyoto, Japan. `https://doi.org/10.1109/icc.2011.5962989`

[34] Mehmet Şükrü Kuran, H. Birkan Yilmaz, Tuna Tugcu, and Ian F. Akyildiz. 2012. Interference effects on modulation techniques in diffusion based nanonetworks. *Elsevier Nano Communication Networks* 3, 1 (March 2012), 65–73. `https://doi.org/10.1016/j.nancom.2012.01.005`

[35] Murat Kuscu, Ergin Dinc, Bilgesu A. Bilgin, Hamideh Ramezani, and Ozgur B. Akan. 2019. Transmitter and Receiver Architectures for Molecular Communications: A Survey on Physical Design With Modulation, Coding, and Detection Techniques. *Proc. IEEE* 107, 7 (July 2019), 1302–1341. `https://doi.org/10.1109/jproc.2019.2916081`

[36] Mohammad U. Mahfuz, Dimitrios Makrakis, and Hussein T. Mouftah. 2014. A Comprehensive Study of Sampling-Based Optimum Signal Detection in Concentration-Encoded Molecular Communication. *IEEE Transactions on NanoBioscience* 13, 3 (Sept. 2014), 208–222. `https://doi.org/10.1109/tnb.2014.2341693`

[37] Mohammad Upal Mahfuz, Dimitrios Makrakis, and Hussein T. Mouftah. 2015. A Comprehensive Analysis of Strength-Based Optimum Signal Detection in Concentration-Encoded Molecular Communication With Spike Transmission. *IEEE Transactions on NanoBioscience* 14, 1 (Jan. 2015), 67–83. `https://doi.org/10.1109/tnb.2014.2368593`

[38] Daniel Tunc McGuiness, Stamatios Giannoukos, Alan Marshall, and Stephen Taylor. 2018. Parameter Analysis in Macro-Scale Molecular Communications Using Advection-Diffusion. *IEEE Access* 6 (May 2018), 46706–46717. `https://doi.org/10.1109/access.2018.2866679`

[39] Daniel Tunc Mcguiness, Stamatios Giannoukos, Alan Marshall, and Stephen Taylor. 2019. Modulation Analysis in Macro-Molecular Communications. *IEEE Access* 7 (Jan. 2019), 11049–11065. `https://doi.org/10.1109/access.2019.2892850`

[40] Michael John Moore, Tatsuya Suda, and Kazuhiro Oiwa. 2009. Molecular Communication: Modeling Noise Effects on Information Rate. *IEEE Transactions on NanoBioscience* (June 2009), 169–180. `https://doi.org/10.1109/TNB.2009.2025039`

[41] Tadashi Nakano, Andrew W. Eckford, and Tokuko Haraguchi.

2013. *Molecular Communication*. Cambridge University Press.

[42] Tadashi Nakano, Y. Okaie, and A. V. Vasilakos. 2013. Transmission Rate Control for Molecular Communication among Biological Nanomachines. *IEEE Journal on Selected Areas in Communications (JSAC)* 31, 12 (Dec. 2013), 835–846. https://doi.org/10.1109/JSAC.2013.SUP2.12130016

[43] Adam Noel, Karen C. Cheung, Robert Schober, Dimitrios Makrakis, and Abdelhakim Hafid. 2017. Simulating with AcCoRD: Actor-based Communication via Reaction–Diffusion. *Elsevier Nano Communication Networks* 11 (March 2017), 44–75. https://doi.org/10.1016/j.nancom.2017.02.002

[44] Jean Philibert. 2006. One and a Half Century of Diffusion: Fick, Einstein, Before and Beyond. *The Open-Access Journal for the Basic Principles of Diffusion Theory, Experiment and Application* 4 (2006), 1–19.

[45] Massimiliano Pierobon and Ian F. Akyildiz. 2010. A physical end-to-end model for molecular communication in nanonetworks. *IEEE Journal on Selected Areas in Communications (JSAC)* 28, 4 (May 2010), 602–611. https://doi.org/10.1109/JSAC.2010.100509

[46] Massimiliano Pierobon and Ian F. Akyildiz. 2011. Diffusion-Based Noise Analysis for Molecular Communication in Nanonetworks. *IEEE Transactions on Signal Processing* 59, 6 (June 2011), 2532–2547. https://doi.org/10.1109/tsp.2011.2114656

[47] Carlos Piñero-Lambea, David Ruano-Gallego, and Luis Ángel Fernández. 2015. Engineered bacteria as therapeutic agents. *Current Opinion in Biotechnology* 35 (Dec. 2015), 94–102. https://doi.org/10.1016/j.copbio.2015.05.004

[48] Xuewen Qian, Marco Di Renzo, and Andrew W. Eckford. 2019. Molecular Communications: Model-Based and Data-Driven Receiver Design and Optimization. *IEEE Access* 7 (Jan. 2019), 53555–53565. https://doi.org/10.1109/access.2019.2912600

[49] Theodore S. Rappaport. 2009. *Wireless Communications: Principles and Practice* (2 ed.). Prentice Hall, Upper Saddle River, NJ.

[50] Amit Kumar Shrivastava, Debanjan Das, and Rajarshi Mahapatra. 2020. Adaptive Threshold Detection and ISI Mitigation in Mobile Molecular Communication. In *IEEE Wireless Communications and Networking Conference (WCNC 2020)*. IEEE, Virtual Conference. https://doi.org/10.1109/wcnc45663.2020.9120603

[51] Christian A. Soldner, Eileen Socher, Vahid Jamali, Wayan Wicke, Arman Ahmadzadeh, Hans-Georg Breitinger, Andreas Burkovski, Kathrin Castiglione, Robert Schober, and Heinrich Sticht. 2020. A Survey of Biological Building Blocks for Synthetic Molecular Communication Systems. *IEEE Communications Surveys & Tutorials* 22, 4 (2020), 2765–2800. https://doi.org/10.1109/comst.2020.3008819

[52] Tatsuya Suda and Tadashi Nakano. 2018. Molecular Communication: A Personal Perspective. *IEEE Transactions on NanoBioscience* 17, 4 (Oct. 2018), 424–432. https://doi.org/10.1109/tnb.2018.2851951

[53] Yin Sun and Benjamin Cyr. 2018. Information Aging Through Queues: A Mutual Information Perspective. In *19th IEEE International Workshop on Signal Processing Advances in Wireless Communications (SPAWC 2018)*. IEEE, Kalamata, Greece. https://doi.org/10.1109/spawc.2018.8445873

[54] Bige D. Unluturk, Derya Malak, and Ozgur B. Akan. 2013. Rate-Delay Tradeoff With Network Coding in Molecular Nanonetworks. *IEEE Transactions on Nanotechnology* 12, 2 (March 2013), 120–128. https://doi.org/10.1109/tnano.2013.2241449

[55] Harald Unterweger, Jens Kirchner, Wayan Wicke, Arman Ahmadzadeh, Doaa Ahmed, Vahid Jamali, Christoph Alexiou, Georg Fischer, and Robert Schober. 2018. Experimental Molecular Communication Testbed Based on Magnetic Nanoparticles in Duct Flow. In *19th IEEE International Workshop on Signal Processing Advances in Wireless Communications (SPAWC 2018)*. Kalamata, Greece, 1–5. https://doi.org/10.1109/SPAWC.2018.8446011

[56] Wayan Wicke, Arman Ahmadzadeh, Vahid Jamali, Harald Unterweger, Christoph Alexiou, and Robert Schober. 2019. Magnetic Nanoparticle-Based Molecular Communication in Microfluidic Environments. *IEEE Transactions on NanoBioscience* 18, 2 (April 2019), 156–169. https://doi.org/10.1109/tnb.2019.2895244

[57] Roy D. Yates and Sanjit K. Kaul. 2019. The Age of Information: Real-Time Status Updating by Multiple Sources. *IEEE Transactions on Information Theory* 65, 3 (March 2019), 1807–1827. https://doi.org/10.1109/tit.2018.2871079

[58] Roy D. Yates, Yin Sun, D. Richard Brown III, Sanjit K. Kaul, Eytan Modiano, and Sennur Ulukus. 2020. *Age of Information: An Introduction and Survey.* cs.IT 2007.08564. arXiv.

[59] H. Birkan Yilmaz, Akif Cem Heren, Tuna Tugcu, and Chan-Byoung Chae. 2014. Three-Dimensional Channel Characteristics for Molecular Communications With an Absorbing Receiver. *IEEE Communications Letters* 18, 6 (June 2014), 929–932. https://doi.org/10.1109/lcomm.2014.2320917